



No slip gravity in light of LISA standard sirens

Alireza Allahyari,^{1,2}★ Rafael C. Nunes³ and David F. Mota⁴

¹School of Astronomy, Institute for Research in Fundamental Sciences (IPM), P. O. Box 19395-5531 Tehran, Iran

²Department of Astronomy and High Energy Physics, Faculty of Physics, Kharazmi University, Tehran, 15719-14911, Iran

³Divisão de Astrofísica, Instituto Nacional de Pesquisas Espaciais, Avenida dos Astronautas 1758, São José dos Campos 12227-010, SP, Brazil

⁴Institute of Theoretical Astrophysics, University of Oslo, P.O. Box 1029 Blindern, N-0315 Oslo, Norway

Accepted 2022 May 21. Received 2022 May 21; in original form 2022 January 10

ABSTRACT

Standard sirens (SS) are the gravitational wave analogue of the astronomical standard candles, and can provide powerful information about the dynamics of the Universe up to very high z values. In this work, we generate three mock SS catalogues based on the merger of massive black hole binaries which are expected to be observed in the LISA operating frequency band. Then, we perform an analysis to test modifications of general relativity (GR) inspired by the no slip gravity framework. We find that in the best scenarios, we can constrain the free parameters which quantify deviations from GR to 21 per cent accuracy, while the Hubble parameter can be simultaneously fit to 6 per cent accuracy. In combination with CMB information, we find a 15 per cent accuracy on the modified gravity free parameters and 0.7 per cent accuracy on the Hubble parameter. The SS events at very large cosmological distances to be observed in LISA band will provide a unique way to test nature of gravity, but in the context of the analysis performed here, it will not be possible to distinguish the no slip gravity from GR.

Key words: gravitation – gravitational waves – cosmology: observations – dark energy.

1 INTRODUCTION

The gravitational wave (GW) astronomy will provide unprecedented opportunity to test fundamental physics. Currently, more than 50 coalescing compact binaries events have already been observed during the three running stages of the LIGO/VIRGO (Abbott et al. 2019, 2021; The LIGO Scientific Collaboration 2021) and other dozens more should be observed in the coming years. Crucially, the observation of the GWs from neutron star binaries GW170817 and its associated electromagnetic counterpart GRB 170817A have marked the dawn of multimessenger cosmology (Soares-Santos et al. 2016; Abbott et al. 2017a, d, c; Arcavi et al. 2017; Goldstein et al. 2017; Savchenko et al. 2017; Tanvir et al. 2017). Such events are dubbed as standard sirens (SS), the gravitational analogue of standard candles (Holz & Hughes 2005; Palmese et al. 2019). The wealth of science that joint detections bring cannot be probed with either messenger alone. Other counterparts like neutrino emissions and polarization features associated to this GW event can shed more light on the nature of the merger (Albert et al. 2017; Shakeri & Allahyari 2018). The importance of such a detection is because the redshift and the location of the source are obtained with more precision breaking the degeneracies in the parameter space. In particular, one appealing application for the SS observations, is the possibility of utilizing events like these to estimate cosmological parameters (Schutz 1986). This provides one complementary probe to constrain cosmological parameters, since the cosmological parameters are encoded in the luminosity distance provided from these events.

An independent measurement of the Hubble constant, H_0 , using the standard siren approach results in $H_0 = 70_{-8}^{12}$ km s⁻¹ Mpc⁻¹

(Abbott et al. 2017b). The errors for one event are still large. However, with the advent of third generation detectors like Einstein Telescope (Maggiore et al. 2020), Cosmic Explorer (Sathyaprakash et al. 2019) which are based on the earth and space-borne detectors like LISA (Luo et al. 2016; Amaro-Seoane et al. 2017; Baker et al. 2019; and TianQin Mei et al. 2021), the constraining power of GWs with electromagnetic counterparts will increase significantly and they could extend these observations to large redshifts. The LISA will operate in the millihertz band with the objective to be an all-sky GW survey (Baker et al. 2019). Science with LISA brings opportunities and challenges in terms of complications which arise because of its motion around the earth. Basically, LISA can be considered as two detectors. It will be launched in three identical drag-free spacecraft forming an equilateral triangle with the arm length of about 2.5×10^6 km (Cutler 1998; Cornish & Rubbo 2003).

The implications of cosmological studies using the standard sirens have motivated focused studies on the nature of dark energy, modified gravity, dark matter, and several other fundamental questions in modern cosmology (Belgacem et al. 2018a, b, 2019; Nishizawa 2018; D’Agostino & Nunes 2019; Nishizawa & Arai 2019; Nunes, Alves & de Araujo 2019; Yang et al. 2019; Baral, Roy & Pal 2020; Belgacem et al. 2020; Bonilla et al. 2020, 2022; Cañas Herrera, Contigiani & Vardanyan 2020, 2021; Dalang, Fleury & Lombriser 2020; Fu et al. 2020; Gray et al. 2020; Lagos & Zhu 2020; Mastrogiovanni, Steer & Barsuglia 2020; Nunes 2020; Wang et al. 2020b, 2022; Yang et al. 2020; Zhang et al. 2020; Baker & Harrison 2021; Bernardo 2021; Cai & Yang 2021; de Souza & Sturani 2021; Ezquiaga et al. 2021; Jiang & Yagi 2021; Kalomenopoulos et al. 2021; Mastrogiovanni et al. 2021a; Matos, Calvão & Waga 2021; Pan et al. 2021; Tasinato et al. 2021; Yang 2021; Zhang & Zhang 2021). Even if the detected event has no electromagnetic counterpart, it is possible to use other methods to study cosmological parameters (Borhanian et al. 2020;

* E-mail: alireza.al@ipm.ir

Wang et al. 2020a; Feeney et al. 2021; Garoffolo et al. 2021; Mastrogiovanni et al. 2021b; Mukherjee, Wandelt & Silk 2021b; Mukherjee et al. 2021a; Zhu et al. 2021).

In this article, we will forecast bounds for a motivated modified gravity model named no slip gravity (Linder 2018), a subclass of the Horndeski gravity model (Horndeski 1974), a general scalar tensor theory with second-order field equations. The main characteristics of no slip model are given by the speed of GWs propagation which is equal to the speed of light, and equality between the effective gravitational coupling strengths to matter and light, but yet different from Newton's constant, which is capable of generating an effective gravitational coupling. Some observational perspectives of this class were previously investigated in Brush, Linder & Zumalacárregui (2019), Mitra et al. (2021), Linder (2020), Brando et al. (2019), Nunes (2020). Our approach is to use the LISA standard sirens to predict the bounds on the no slip gravity baseline parameters. In following analysis, we integrate the modified luminosity distance from standard sirens to constrain the main free parameters of the model. Also, we combine our results with previous results where cosmic microwave background data were used for no slip gravity, to get tight constraints on the model.

This work is organized as follows. In Section 2, we present the modified luminosity distance in our model. Section 3 is devoted to the LISA standard sirens where we show how we generate the mock data. In Section 4, we present our main results. Finally, our final remarks are included in Section 5.

2 PROPAGATION OF GRAVITATIONAL WAVES IN MODIFIED GRAVITY

One particular way by which modified theories leave their imprints on the cosmological observables is the modified propagation equations for the tensorial part of the perturbations. This leads to a notion of GW luminosity distance different from the electromagnetic luminosity distance. This provides an arena to test the modified theories in the context of GWs by the standard sirens, the GW events with the associated electromagnetic counterparts. The standard expression of the luminosity distance in a universe with matter density fraction Ω_m , radiation density fraction Ω_R and dark energy density ρ_{de} is defined as

$$d_L^{em}(z) = \frac{1+z}{H_0} \int_0^z \frac{dz'}{E(\tilde{z})}, \quad (1)$$

where

$$E(z) = \sqrt{\Omega_R(1+z)^4 + \Omega_m(1+z)^3 + \rho_{de}(z)/\rho_0}, \quad (2)$$

where we have $\rho_0 = 3H_0^2/(8\pi G)$ (Belgacem et al. 2018a). In GR the transverse traceless part of metric perturbations, $\partial_i h^{ij} = h_i^i = 0$, produces the gravitational waves. The propagation equation for GWs on a flat FRW background in absence of anisotropic stress tensor for the polarization A is given by

$$h''_A + 2\mathcal{H}h'_A + k^2h_A = 0, \quad A = +, \times \quad (3)$$

where the prime denotes derivative with respect to the conformal time and $\mathcal{H} = a'/a$. Defining

$$h_A(\eta, k) = \frac{\chi_A(\eta, k)}{a(\eta)}, \quad (4)$$

we find that

$$\chi''_A(\eta, k) + \left(k^2 - \frac{a''}{a}\right)\chi_A(\eta, k) = 0. \quad (5)$$

This shows that the amplitude of gravitational waves decrease as $1/a$ and in GR the luminosity distance for the gravitational waves from a binary is the same as electromagnetic waves $d_L^{em} = d_L^{gw}$. In a generic modified theory the equation for GWs in the Fourier space reads as

$$h''_A + 2\mathcal{H}[1 - \delta(\eta)]h'_A + k^2h_A = 0. \quad (6)$$

We have neglected the modulations in k^2 term as they change the speed of GWs and we assume the vacuum field equations. Changing the speed of GWs is not favoured given the stringent limit set by GW170817 $|c_{gw} - c|/c < O(10^{-15})$. To solve equation (6) one introduces

$$h_A(\eta, k) = \frac{\chi_A(\eta, k)}{\bar{a}(\eta)}, \quad (7)$$

$$\frac{\bar{a}'}{\bar{a}} = \mathcal{H}(1 - \delta(\eta)). \quad (8)$$

This way one finds that the luminosity distance for the GWs obeys a different equation. We have (Belgacem et al. 2018a; Hogg, Martinelli & Nesseris 2020; Finke et al. 2021; Mastrogiovanni et al. 2021a),

$$d_L^{gw}(z) = d_L^{em}(z) \exp \left\{ - \int_0^z \frac{dz'}{1+z'} \delta(z') \right\}. \quad (9)$$

The modified gravity we consider which changes the propagation of GWs as we have in equations (6) and (9) is the no slip model. This modified theory has the advantage of not changing the propagation speed for GWs. Therefore, it is favoured by the current observations. This model exhibits simple behaviour in terms of phenomenological parametrizations and has been applied to study the CMB (Brush et al. 2019).

No slip model belongs to the well-motivated larger class of Horndeski scalar-tensor theories (Horndeski 1974). The Horndeski is the most general scalar-tensor theory with second-order equations of motion in four dimensions from which different modified theories can be obtained such as Quintessence, k-essence, and $f(R)$ gravity. The Lagrangian for the theory is presented in Refs. Kobayashi (2019), Gleyzes, Langlois & Vernizzi (2015) and other references therein. This theory can be tuned such that GWs propagate at the speed of light to conform with the limit set by GW170817. Moreover, a very important prediction of modified gravity theories is the modification of Einstein equations in a way where the coupling of gravity to matter and light could be different. In other words, the Poisson equation and the lensing equation have different dependence on the metric perturbations. The perturbations on the FRW background in the conformal Newtonian gauge are given by

$$ds^2 = a(\eta)^2 \{ -(1+2\Psi)d\eta^2 + (1-2\Phi)\delta_{ij}dx^i dx^j \}, \quad (10)$$

where Φ and Ψ are metric perturbations. It is usually a combination, $\Phi + \Psi$, which appears in the geodesic equations for photons (Bertacca, Maartens & Clarkson 2014; Allahyari & Firouzjaee 2017). More explicitly, the Einstein equations take the form

$$\nabla^2\Psi = 4\pi a^2 G_N G_{matter} \rho_m \delta_m \quad (11)$$

$$\nabla^2(\Psi + \Phi) = 8\pi a^2 G_N G_{light} \rho_m \delta_m, \quad (12)$$

where the quantity ρ_m is the background matter density, and $\delta_m = \delta\rho_m/\rho_m$ is the comoving density perturbation and G_{light} and G_{matter} are functions of time and G_N is the gravitational constant.

To quantify the effect of gravity on matter and photons the gravitational slip parameter is defined by

$$\eta = \frac{G_{matter}}{G_{light}}. \quad (13)$$

In the no slip model the gravitational interaction is gauged so that for the gravitational slip parameter we have $\eta = 1$. This way, we find that the effective gravitational couplings are simply related by

$$G_{\text{matter}} = G_{\text{light}} = \frac{m_p^2}{M_*^2}, \quad (14)$$

where m_p and M_* are Planck and time-dependent Planck mass, respectively. M_* is a function of the terms in the Horndeski Lagrangian Kase & Tsujikawa (2019), Linder, Sengör & Watson (2016). We find that the gravitational coupling strength is modified. Therefore, the growth of structures and lensing potentials will deviate from GR prediction.

The other condition to impose on the Horndeski model to derive no slip model is the speed of GWs. The Horndeski model can accommodate different propagation speeds for GWs than the speed of light. In Horndeski model the second order action for tensorial perturbations reads as

$$S_{\text{tensor}}^{(2)} = \frac{1}{8} \int d^3 q_t \left[\dot{h}_{ij}^2 - \frac{c_{gw}^2}{a^2} (\partial_k h_{ij})^2 \right] dt d^3 x, \quad (15)$$

where q_t is defined in Ref. Kase & Tsujikawa (2019). The speed of tensorial perturbations is given by c_{gw} which is function of various terms in the Horndeski Lagrangian.

In no slip model, we impose the condition to have $c_{gw} = 1$. Varying the action in equation (15) and imposing the conditions mentioned, we get

$$\ddot{h}_A + \left(3H + \frac{\dot{q}_t}{q_t} \right) \dot{h}_A + \frac{k^2}{a^2} h_A = 0. \quad (16)$$

This way we find that $G_{\text{matter}} = G_{\text{light}} = 1/(16\pi G_N G_4)$ and $q_t = 2G_4 = M_*^2$, where G_4 is one of the terms in the Horndeski Lagrangian (Kase & Tsujikawa 2019). Comparing equations (16) and (6), we have $-2\delta = \frac{d \ln q_t}{d \ln a}$. We find that it is the running of the Planck mass which controls the tensor perturbations in this theory. At this point, one could define a simple phenomenological parametrization to capture the main features of the theory. One could start with a parametrization for δ or M_* . As we are interested in studying the GW luminosity distance we take the first approach, namely δ parametrization. Specializing to our case study here, no slip model, we also use the phenomenological parametrization introduced by Belgacem et al. (2019)

$$\delta(z) = \frac{n(1-\xi)}{1-\xi+\xi(1+z)^n}, \quad (17)$$

where ξ and n are constants. This parametrization is applicable to models in which we expect some simple properties in low and high redshifts. More explicitly, we find that at the high redshifts $z \rightarrow \infty$, we have $\delta(z) \rightarrow 0$. Moreover, when $z \rightarrow 0$, this yields $\delta(z) \rightarrow n(1-\xi)$, where for $\xi = 1$ we have $\delta(z) \rightarrow 0$. Thus, we recover the standard expression for the luminosity distance at high and low redshifts. We expect this parametrization to be a viable parametrization as theory is not complicated. Please also note that in models where there are also other degrees of freedom other than one scalar field, the parametrization in equation (17) might not capture the details of the theory. Examples where this parametrization might not work are bigravity theories (Comelli, Crisostomi & Pilo 2012; Hassan & Rosen 2012). Alternatively, another parametrization starting with variation of Planck mass is given in Refs. Brush et al. (2019), Mitra et al. (2021),

$$\left(\frac{m_p}{M_*} \right)^{-2} = 1 + \frac{\mu}{1 + (\frac{a}{a_t})^{-\tau}}, \quad (18)$$

where μ is the amplitude of transition, a_t is the scale factor at the transition time, and τ is the rapidity. This parametrization has a simple transition from unity in the past to some constant value in the future. We find that simple parametrizations of the model are adequate for no slip model. Here, we find it more convenient to work in n, ξ parametrization, as defined in equation (17). For the sake of comparison, the mapping from set (n, ξ) to set (τ, μ) has been provided in Ref. Mitra et al. (2021)

$$\xi = \lim_{z \rightarrow \infty} \frac{M_*(0)}{M_*(z)}, \quad (19)$$

$$n \simeq \frac{\alpha_{M0}}{2(\xi - 1)}, \quad (20)$$

where $\alpha_{M0} = -2\delta(0)$. One could check that the mapping generates the same behaviour for $\delta(z)$ in two parametrizations. The parametrization in equation (18) was suggested to produce a stable and ghost-free model. Therefore, this mapping ensures that parametrization in equation (17) is a good choice.

3 LISA STANDARD SIRENS

LISA is a space-borne detector with its sensitivity peak around 1 millihertz. Among astrophysical sources LISA can reach including galactic binaries (Korol et al. 2017; Breivik et al. 2018), stellar-origin black hole binaries (Sesana 2016), and extreme-mass-ratio inspirals (Babak et al. 2017), LISA will also observe massive black hole binaries (MBHBs) from 10^4 to 10^7 solar masses (Klein et al. 2016). The high signal-to-noise ratio (SNR) of the detected signals will allow for more precise parameter estimations. Among the most probable LISA sources with electromagnetic counterparts are MBHBs. In particular, MBHBs are supposed to merge in gas-rich environments and within the LISA frequency band allowing for electromagnetic followups to determine their redshifts. The prospect of MBHBs which could have EM counterparts extends up to $z \sim 7$ providing a unique probe of the Universe at high redshifts (Klein et al. 2016).

Our catalogue is based on the model in Ref. Tamanini et al. (2016) where they use a semi-analytic model which allows tracing the galactic baryonic structures and dark matter mergers. In addition, the model integrates the black hole seeding at high redshifts and the delays between the merger of two galaxies and that of the massive BHs residing in the galaxies.

Theoretical models and simulations can predict the redshift distribution and merger rate of MBHBs. Depending on the initial conditions for black hole formation at high redshifts, there are two scenarios light seed and heavy seed. In the light seed scenario massive BHs are assumed to grow from the remnants of population III (pop III) stars forming at $z \approx 15-20$. In the heavy seed scenario, the massive BHs are assumed to form from the collapse of protogalactic discs (Tamanini et al. 2016). The result of the scenarios produce three categories of population models named Pop III, Delay and No Delay (Madau & Rees 2001; Volonteri, Lodato & Natarajan 2008; Klein et al. 2016). Among all the merger events, one chooses the events with an SNR threshold and localization error $\Delta\Omega$. The redshift distribution of sources based on LISA sensitivity is reported in Ref. Tamanini et al. (2016), Tamanini (2017).

For each source one then calculates the associated GW luminosity distance assuming a given cosmology. We need to consider the prospective errors on d_L based on the LISA sensitivity. Using the criteria in Ref. Speri et al. (2021) where they use the results of Ref. Marsat, Baker & Dal Canton (2021) to fix the proportionality

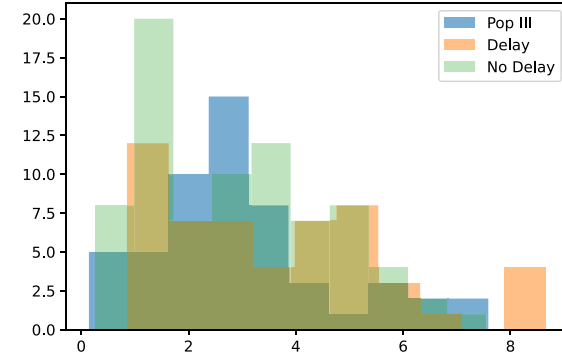


Figure 1. Redshift distribution of MBHB standard sirens, namely, Pop III, Delay, and No Delay.

factor in the approximation $\sigma_{\text{LISA}}/d_L \propto 2d_L$, we have

$$\frac{\sigma_{\text{LISA}}(z)}{d_L(z)} = 0.05 \left(\frac{d_L(z)}{36.6 \text{ Gpc}} \right). \quad (21)$$

However, this will give us the instrument error. We also need to consider three pieces of ingredients in our error estimation (Speri et al. 2021; Wang et al. 2022). They are weak lensing

$$\sigma_{\text{dels}}(z) = F_{\text{dels}}(z)\sigma_{\text{lens}}(z), \quad (22)$$

where we have

$$F_{\text{dels}}(z) = 1 - \frac{0.3}{\pi/2} \arctan \left(\frac{z}{z_*} \right), \quad (23)$$

$$\frac{\sigma_{\text{lens}}(z)}{d_L(z)} = 0.066 \left(\frac{1 - (1+z)^{-0.25}}{0.25} \right)^{1.8}, \quad (24)$$

peculiar velocity

$$\frac{\sigma_v(z)}{d_L(z)} = \left[1 + \frac{c(1+z)^2}{H(z)d_L(z)} \right] \frac{\sqrt{\langle v^2 \rangle}}{c}, \quad (25)$$

with $\langle v^2 \rangle = 500 \text{ km s}^{-1}$, and redshift measurement error (Speri et al. 2021)

$$\sigma_{\text{photo}}(z) = 0.03(1+z) \quad \text{if } z > 2. \quad (26)$$

The total error is given by adding in quadrature all contributions:

$$(\sigma_{d_L})^2 = (\sigma_{\text{photo}})^2 + (\sigma_{\text{lens}})^2 + (\sigma_{\text{LISA}})^2 + (\sigma_v)^2. \quad (27)$$

We generate three catalogues based on these criteria for the aforementioned distributions, namely, Pop III, Delay and No Delay for a ten-year mission. We generate our mock catalogue from a fiducial input baseline with $H_0 = 67.4 \text{ km s}^{-1} \text{ Mpc}^{-1}$, $\Omega_m = 0.315$, $\xi = 1.0328$, $n = 0.3176$. The pair values (ξ, n) are chosen in order to generate a mock catalogue using modified gravity corrections. The motivation for this choice meets in the sense that we do not assume the generation of the full simulated catalogues fixed on the ΛCDM baseline. Since we are interested in investigating deviations from the standard cosmology, we choose some minimal input deviation from ΛCDM cosmology to create the mock data. Then, the forecast of experiments, in this case, the LISA mission, will quantify the expected error bar on the baseline of the model. Note that our choice for the pair values (ξ, n) is compatible with current constraints (Brush et al. 2019; Mitra et al. 2021).

Fig. 1 shows the redshift distributions of the mock catalogues and Fig. 2 shows the luminosity distance and the corresponding errors based on our input baseline, as well as the three categories of LISA SS sources. In what follows, we will analyse the free parameters of the theory and present our main results.

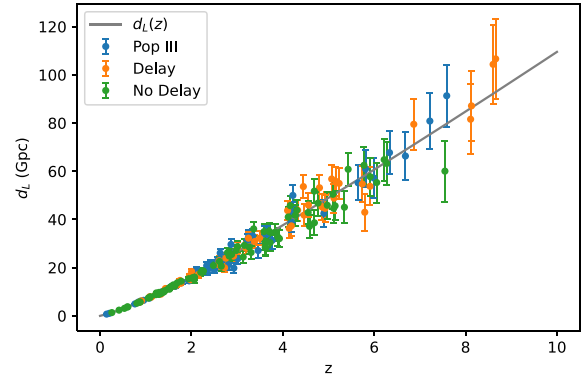


Figure 2. LISA standard sirens at all redshifts from the three population models we consider in this work.

Table 1. Constraints at 68 per cent CL from the Pop III samples and their combination with CMB information.

Parameter	Pop III	Pop III + CMB
$H_0 (\text{km s}^{-1} \text{ Mpc}^{-1})$	66.71 ± 0.95	66.92 ± 0.56
Ω_m	0.31 ± 0.11	0.3160 ± 0.0070
n	$0.64^{+0.56}_{-0.68}$	$0.15^{+0.69}_{-0.80}$
ξ	0.98 ± 0.33	$1.016^{+0.069}_{-0.083}$

Table 2. Same as Table 1, but for the delay samples.

Parameter	Delay	Delay + CMB
$H_0 (\text{km s}^{-1} \text{ Mpc}^{-1})$	70.8 ± 4.5	67.78 ± 0.91
Ω_m	$0.456^{+0.049}_{-0.13}$	0.3098 ± 0.0092
n	0.98 ± 0.55	$0.42^{+0.47}_{-0.78}$
ξ	$1.362^{+0.081}_{-0.22}$	$1.13^{+0.14}_{-0.34}$

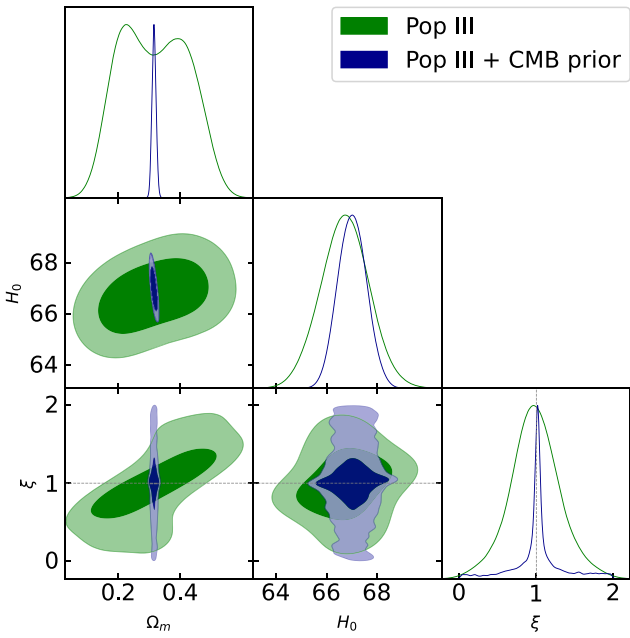
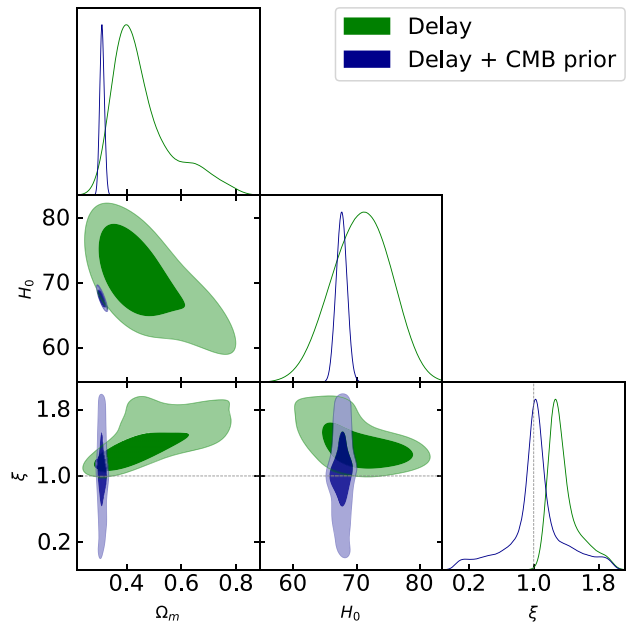
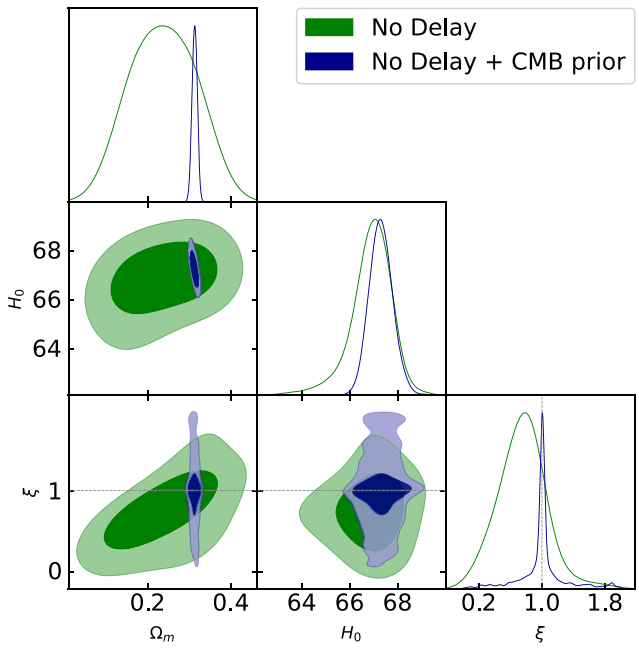
4 RESULTS AND DISCUSSION

In this section, we present our main results on the model parameters by performing Bayesian Monte Carlo Markov Chain analysis. We create new likelihoods in `MontePython` code (Audren et al. 2013) to analyse the SS mock data as presented above. Then, we use the Metropolis–Hastings mode in `CLASS + MontePython` code (Blas, Lesgourgues & Tram 2011; Audren et al. 2013; Brinckmann & Lesgourgues 2019) to derive the constraints on cosmological parameters ensuring a Gelman–Rubin convergence criterion of $R - 1 < 10^{-3}$ (Gelman & Rubin 1992). We divide our analysis as follows: First, we will analyse our baseline for each category of populations as defined in Section 3, namely, Pop III, Delay, and No Delay samples. Then, we will do a joint analysis using the CMB information as obtained in the context of no slip gravity in Ref. Brush et al. (2019). We simulate LISA + CMB constraints on the no slip gravity adding appropriate Gaussian priors on the parameters H_0 and w_{cdm} as derivatives in Ref. Brush et al. (2019).

We summarize the main results of our statistical analysis in Tables 1, 2, and 3 for the cases with Pop III, Delay, and No Delay mock data, respectively. The tables also show the best fit for LISA + CMB prior combination. Figs 3, 4, and 5 show the 2D joint posterior distributions at 68 per cent CL and 95 per cent CL for some parameters of interest. As expected by the definition in equation (17), we note that the parameters n and ξ are completely degenerate statistically. In all our analysis, we choose to keep both parameters free, although only the parameter ξ would suffice to quantify the deviations of GR. Fig. 6

Table 3. Same as Table 1, but for the no delay samples.

Parameter	No delay	No delay + CMB
H_0 ($\text{km s}^{-1} \text{Mpc}^{-1}$)	$66.87^{+0.92}_{-0.63}$	67.21 ± 0.47
Ω_m	0.238 ± 0.078	0.3133 ± 0.0062
n	$0.43^{+0.37}_{-0.55}$	$0.07^{+0.71}_{-0.54}$
ξ	0.75 ± 0.31	$1.037^{+0.076}_{-0.17}$

**Figure 3.** 1D posterior distributions and 2D joint contours for the parameter space H_0 , Ω_m , and ξ for LISA Pop III samples and Pop III + CMB prior. The $\xi = 1$ prediction recovers the GR.**Figure 4.** Same as in Fig. 3, but for the delay samples.**Figure 5.** Same as in Fig. 3, but for the no delay samples.

shows the 1D marginalized posterior probability distributions for the parameter n .

We find that the free parameter which quantifies deviation of GR, ξ , can be measured with 33 per cent, 21 per cent, and 41 per cent accuracy from the Pop III, Delay, and No Delay populations, respectively. As already pointed out in Mitra et al. (2021), we see a significant degeneracy between the parameters ξ and n , which on the other hand is also very degenerate with the matter density Ω_m and the Hubble constant, H_0 . Note that for $n = 0$, or equivalently $\xi = 1$, the equations of the model also reduce to GR. It is interesting to note that the parameter ξ is positively correlated with Ω_m , and does not show significant correlation with H_0 . As the matter density increases, the luminosity distance to the different GWs sources will decrease, but this can be balanced by increasing the effects from the modified gravity model. We find that the Hubble parameter can be simultaneously fit to 1.4 per cent, 6.2 per cent, and 1.1 per cent accuracy from the Pop III, Delay, and No Delay populations, respectively.

To test gravity through the propagation of gravitational waves is a unique probe, though the model cannot be distinguished due to strong degeneracy in the whole parameter space using only the SS events. Therefore, in this case, it will be important to combine the SS sample with other probes. Geometrical probes measured by electromagnetic waves like Supernovae Type Ia, Baryon Acoustic Oscillation distance, cosmic chronometers, among others, are insensitive on the no slip gravity free parameters, but can provide independent constraints on the Ω_m and H_0 , and then to help break this degeneracy on ξ and n . On the other hand, the no slip gravity prediction is sensitive to the amplitude of late-time matter fluctuations (weak-lensing and redshift-space distortions measurements) and CMB anisotropies. As defined previously, we combine the MBHB standard sirens populations with CMB prior information in order to have a forecast of how much this combination can improve the precision on the parametric space. Taking LISA + CMB prior, we note a 20 per cent, 33 per cent, and 15 per cent accuracy from the Pop III, Delay, and No Delay populations, respectively. Moreover, H_0 can be simultaneously

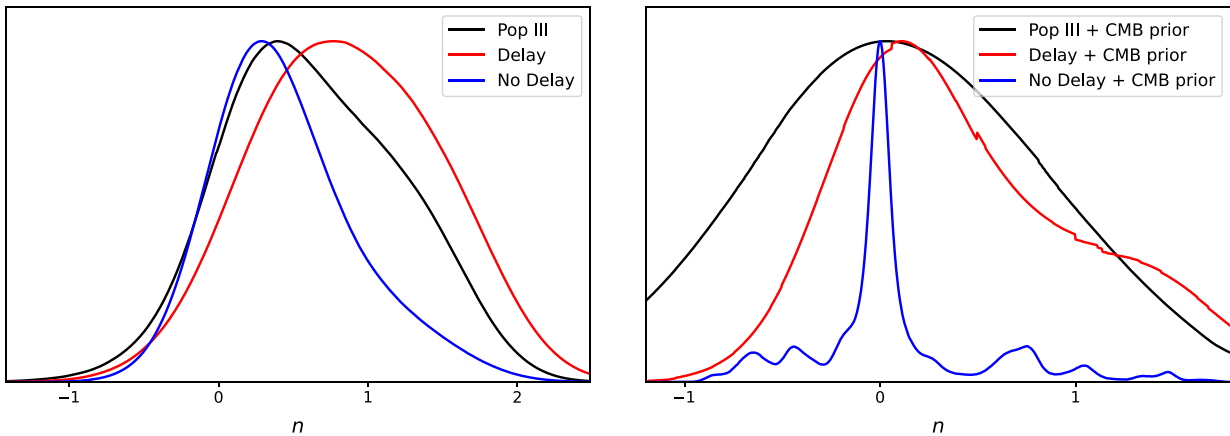


Figure 6. 1D marginalized posterior probability distributions for n , obtained for each LISA mock sample on the left-hand panel and in combination with CMB prior on the right-hand panel.

fit to 0.8 per cent, 1.2 per cent, and 0.7 per cent accuracy from the Pop III, Delay, and No Delay populations, respectively. Note that the cases Delay and No Delay populations, generate higher and lower values for Ω_m , respectively, when compared with the value observed by CMB. On the other hand, the parameter ξ cannot be measured via electromagnetic waves probes as discussed earlier. Any possible improvements on ξ will happen by breaking the degeneracy on the other parameters, in special Ω_m , because ξ and Ω_m are correlated with each other. When we add the CMB prior, the pair (Ω_m, H_0) tends to $(0.31, 67.4)$. Looking at the parametric space $\xi - \Omega_m$ (see Figs 4, 5), we can notice this effect. Therefore, the compression on Ω_m to Planck values, can increase the relative error on ξ in some cases. We note it more significantly in the Delay case. A way to robustly improve the total constraint on ξ would be to combine our analysis with weak lensing and redshift-space distortions measurements. Because in this case, all probes are very sensitive to ξ effects. These steps will be left for future perspectives.

We have extended the analysis in Ref. Mitra et al. (2021) considering mock data from the LISA perspective. We see an overall improvement on the precision of the Hubble constant, H_0 , and Ω_m by including the CMB information. However, we see that by including the CMB it is difficult to distinguish the model from GR as the 68 per cent credible intervals on n and ξ in Tables 1, 2, and 3 contain the GR prediction, namely $\xi = 1$. We note the prospective strength of implementing the CMB is that the degeneracy between ξ and Ω_m can be broken.

5 FINAL REMARKS

We have presented a forecast analysis for the standard siren events which are expected to be observed in LISA frequency band for three categories of population models, named, Pop III, Delay, and No Delay. Then, we performed a parameter estimation analysis to test modifications of GR inspired by the no slip gravity, where the speed of GWs propagation is equal to the speed of light, and the effective gravitational coupling strengths to matter and light are equal, but yet different from Newton's constant coupling.

In our analysis we have also included the priors from the CMB and find that perspectives towards no slip gravity can be well tested within the expected perspective for cosmological observations with LISA. Adding the CMB information could help improve our parameter

estimation and the shape of covariances in the parameter space. In combination with CMB information, we find a 15 per cent accuracy on the modified gravity free parameters and 0.7 per cent accuracy on the Hubble parameter.

In this work we have considered one space-borne detector. A more sophisticated future study will be to include both LISA and TianQin or Taiji Ruan et al. (2020). This could increase the number of the GW events with electromagnetic counterparts and improve the whole parameter space of the model. In the next decades GW detectors will form a powerful detector network. This will allow us to do joint detections for events. This can be utilized to do complementary studies of modified gravity theories with modified GW propagation equations. On the other hand, the modified GW propagation arises naturally from any modified gravity theory. It may be interesting to search and improve the expected study of LISA sources without electromagnetic counterpart, and use these information to test modified GW propagation, since several LISA sources are expected at large cosmological distance (Borhanian et al. 2020; Wang et al. 2020a; Feeney et al. 2021; Mukherjee et al. 2021b). Thus, we can significantly increase our sample, number of events for doing statistics. Also, it may be interesting to search the modified GW propagation effects on the gravitational wave background signal expected in LISA band (Kowalska, Bulik & Belczynski 2012; D’Orazio & Samsing 2018; Samsing & D’Orazio 2018).

ACKNOWLEDGEMENTS

The authors thank the referee for some useful comments that improved the manuscript. RCN acknowledges financial support from the Fundação de Amparo à Pesquisa do Estado de São Paulo (FAPESP, São Paulo Research Foundation) under the project No. 2018/18036-5. DFM thanks the Research Council of Norway for their support. Some computations were performed on resources provided by UNINETT Sigma2 – the National Infrastructure for High Performance Computing and Data Storage in Norway.

DATA AVAILABILITY

The data underlying this article will be shared on reasonable request to the corresponding author.

REFERENCES

- Abbott R. et al., 2021, *Phys. Rev. X*, 11, 021053
 Abbott B. P. et al., 2017a, *Phys. Rev. Lett.*, 119, 161101
 Abbott B. P. et al., 2017b, *Nature*, 551, 85
 Abbott B. P. et al., 2017c, *ApJ*, 848, L12
 Abbott B. P. et al., 2017d, *ApJ*, 848, L13
 Abbott B. P. et al., 2019, *Phys. Rev. X*, 9, 031040
 Albert A. et al., 2017, *ApJ*, 850, L35
 Allahyari A., Firouzjaee J. T., 2017, *Phys. Rev. D*, 95, 063519
 Amaro-Seoane P. et al., 2017, preprint ([arXiv:1702.00786](https://arxiv.org/abs/1702.00786))
 Arcavi I. et al., 2017, *Nature*, 551, 64
 Audren B., Lesgourgues J., Benabed K., Prunet S., 2013, *J. Cosmol. Astropart. Phys.*, 02, 001
 Babak S. et al., 2017, *Phys. Rev. D*, 95, 103012
 Baker J. et al., 2019, preprint ([arXiv:1907.06482](https://arxiv.org/abs/1907.06482))
 Baker T., Harrison I., 2021, *J. Cosmol. Astropart. Phys.*, 01, 068
 Baral P., Roy S. K., Pal S., 2020, *MNRAS*, 500, 2896
 Belgacem E. et al., 2019, *J. Cosmol. Astropart. Phys.*, 07, 024
 Belgacem E., Dirian Y., Foffa S., Maggiore M., 2018a, *Phys. Rev. D*, 97, 104066
 Belgacem E., Dirian Y., Foffa S., Maggiore M., 2018b, *Phys. Rev. D*, 98, 023510
 Belgacem E., Foffa S., Maggiore M., Yang T., 2020, *Phys. Rev. D*, 101, 063505
 Bernardo R. C., 2021, *Phys. Rev. D*, 104, 024070
 Bertacca D., Maartens R., Clarkson C., 2014, *J. Cosmol. Astropart. Phys.*, 11, 013
 Blas D., Lesgourgues J., Tram T., 2011, *J. Cosmol. Astropart. Phys.*, 07, 034
 Bonilla A., D'Agostino R., Nunes R. C., de Araujo J. C. N., 2020, *J. Cosmol. Astropart. Phys.*, 03, 015
 Bonilla A., Kumar S., Nunes R. C., Pan S., 2022, *MNRAS*, 512, 4231
 Borhanian S., Dhani A., Gupta A., Arun K. G., Sathyaprakash B. S., 2020, *ApJ*, 905, L28
 Brando G., Falciano F. T., Linder E. V., Velten H. E. S., 2019, *J. Cosmol. Astropart. Phys.*, 11, 018
 Breivik K., Kremer K., Bueno M., Larson S. L., Coughlin S., Kalogera V., 2018, *ApJ*, 854, L1
 Brinckmann T., Lesgourgues J., 2019, *Phys. Dark Univ.*, 24, 100260
 Brush M., Linder E. V., Zumalacárregui M., 2019, *J. Cosmol. Astropart. Phys.*, 01, 029
 Cai R.-G., Yang T., 2021, *J. Cosmol. Astropart. Phys.*, 12, 017
 Cañas Herrera G., Contigiani O., Vardanyan V., 2020, *Phys. Rev. D*, 102, 043513
 Cañas Herrera G., Contigiani O., Vardanyan V., 2021, *ApJ*, 918, 20
 Comelli D., Crisostomi M., Pilo L., 2012, *J. High Energy Phys.*, 06, 085
 Cornish N. J., Rubbo L. J., 2003, *Phys. Rev. D*, 67, 022001
 Cutler C., 1998, *Phys. Rev. D*, 57, 7089
 D'Agostino R., Nunes R. C., 2019, *Phys. Rev. D*, 100, 044041
 D'Orazio D. J., Samsing J., 2018, *MNRAS*, 481, 4775
 Dalang C., Fleury P., Lombriser L., 2020, *Phys. Rev. D*, 102, 044036
 de Souza J. M. S., Sturani R., 2021, *Phys. Dark Univ.*, 32, 100830
 Ezquiaga J. M., Hu W., Lagos M., Lin M.-X., 2021, *J. Cosmol. Astropart. Phys.*, 11, 048
 Feeney S. M., Peiris H. V., Nissanke S. M., Mortlock D. J., 2021, *Phys. Rev. Lett.*, 126, 171102
 Finke A., Foffa S., Iacobelli F., Maggiore M., Mancarella M., 2021, *J. Cosmol. Astropart. Phys.*, 08, 026
 Fu X., Yang J., Chen Z., Zhou L., Chen J., 2020, *Eur. Phys. J. C*, 80, 893
 Garoffolo A., Raveri M., Silvestri A., Tasinato G., Carbone C., Bertacca D., Matarrese S., 2021, *Phys. Rev. D*, 103, 083506
 Gelman A., Rubin D. B., 1992, *Stat. Sci.*, 7, 457
 Gleyzes J., Langlois D., Vernizzi F., 2015, *Int. J. Mod. Phys. D*, 23, 1443010
 Goldstein A. et al., 2017, *ApJ*, 848, L14
 Gray R. et al., 2020, *Phys. Rev. D*, 101, 122001
 Hassan S. F., Rosen R. A., 2012, *J. High Energy Phys.*, 02, 126
 Hogg N. B., Martinelli M., Nesseris S., 2020, *J. Cosmol. Astropart. Phys.*, 12, 019
 Holz D. E., Hughes S. A., 2005, *ApJ*, 629, 15
 Horndeski G. W., 1974, *Int. J. Theor. Phys.*, 10, 363
 Jiang N., Yagi K., 2021, *Phys. Rev. D*, 103, 124047
 Kalomenopoulos M., Khochfar S., Gair J., Arai S., 2021, *MNRAS*, 503, 3179
 Kase R., Tsujikawa S., 2019, *Int. J. Mod. Phys. D*, 28, 1942005
 Klein A. et al., 2016, *Phys. Rev. D*, 93, 024003
 Kobayashi T., 2019, *Rep. Prog. Phys.*, 82, 086901
 Korol V., Rossi E. M., Groot P. J., Nelemans G., Toonen S., Brown A. G. A., 2017, *MNRAS*, 470, 1894
 Kowalska I., Bulik T., Belczynski K., 2012, *A&A*, 541, A120
 Lagos M., Zhu H., 2020, *J. Cosmol. Astropart. Phys.*, 06, 061
 Linder E. V., 2018, *J. Cosmol. Astropart. Phys.*, 03, 005
 Linder E. V., 2020, *J. Cosmol. Astropart. Phys.*, 10, 042
 Linder E. V., Sengör G., Watson S., 2016, *J. Cosmol. Astropart. Phys.*, 05, 053
 Luo J. et al., 2016, *Class. Quantum Gravity*, 33, 035010
 Madau P., Rees M. J., 2001, *ApJ*, 551, L27
 Maggiore M. et al., 2020, *J. Cosmol. Astropart. Phys.*, 03, 050
 Marsat S., Baker J. G., Dal Canton T., 2021, *Phys. Rev. D*, 103, 083011
 Mastrogiovanni S. et al., 2021b, *Phys. Rev. D*, 104, 062009
 Mastrogiovanni S., Steer D., Barsuglia M., 2020, *Phys. Rev. D*, 102, 044009
 Mastrogiovanni S., Haegel L., Karathanasis C., Hernandez I. M. n., Steer D. A., 2021a, *J. Cosmol. Astropart. Phys.*, 02, 043
 Matos I. S., Calvão M. O., Waga I., 2021, *Phys. Rev. D*, 103, 104059
 Mei J. et al., 2021, *Progr. Theor. Exp. Phys.*, 2021, 05A107
 Mitra A., Mifsud J., Mota D. F., Parkinson D., 2021, *MNRAS*, 502, 5563
 Mukherjee S., Wandelt B. D., Nissanke S. M., Silvestri A., 2021a, *Phys. Rev. D*, 103, 043520
 Mukherjee S., Wandelt B. D., Silk J., 2021b, *MNRAS*, 502, 1136
 Nishizawa A., 2018, *Phys. Rev. D*, 97, 104037
 Nishizawa A., Arai S., 2019, *Phys. Rev. D*, 99, 104038
 Nunes R. C., 2020, *Phys. Rev. D*, 102, 024071
 Nunes R. C., Alves M. E. S., de Araujo J. C. N., 2019, *Phys. Rev. D*, 100, 064012
 Palmese A. et al., 2019, *Bull. Am. Astron. Soc.*, 51, 310
 Pan Y., He Y., Qi J., Li J., Cao S., Liu T., Wang J., 2021, *ApJ*, 911, 135
 Ruan W.-H., Guo Z.-K., Cai R.-G., Zhang Y.-Z., 2020, *Int. J. Mod. Phys. A*, 35, 2050075
 Samsing J., D'Orazio D. J., 2018, *MNRAS*, 481, 5445
 Sathyaprakash B. et al., 2019, *Bull. Am. Astron. Soc.*, 51, 248
 Savchenko V. et al., 2017, *ApJ*, 848, L15
 Schutz B. F., 1986, *Nature*, 323, 310
 Sesana A., 2016, *Phys. Rev. Lett.*, 116, 231102
 Shakeri S., Allahyari A., 2018, *J. Cosmol. Astropart. Phys.*, 11, 042
 Soares-Santos M. et al., 2016, *ApJ*, 823, L33
 Speri L., Tamanini N., Caldwell R. R., Gair J. R., Wang B., 2021, *Phys. Rev. D*, 103, 083526
 Tamanini N., 2017, *J. Phys. Conf. Ser.*, 840, 012029
 Tamanini N., Caprini C., Barausse E., Sesana A., Klein A., Petiteau A., 2016, *J. Cosmol. Astropart. Phys.*, 04, 002
 Tanvir N. R. et al., 2017, *ApJ*, 848, L27
 Tasinato G., Garoffolo A., Bertacca D., Matarrese S., 2021, *J. Cosmol. Astropart. Phys.*, 06, 050
 The LIGO Scientific Collaboration, 2021, preprint ([arXiv:2108.01045](https://arxiv.org/abs/2108.01045))
 Volonteri M., Lodato G., Natarajan P., 2008, *MNRAS*, 383, 1079
 Wang R., Ruan W.-H., Yang Q., Guo Z.-K., Cai R.-G., Hu B., 2022, *Natl. Sci. Rev.*, 9, 2
 Wang L.-F., Zhao Z.-W., Zhang J.-F., Zhang X., 2020b, *J. Cosmol. Astropart. Phys.*, 11, 012
 Wang L.-F., Jin S.-J., Zhang J.-F., Zhang X., 2022, *Sci. China Phys. Mech. Astron.*, 65, 210411
 Yang T., 2021, *J. Cosmol. Astropart. Phys.*, 05, 044

- Yang W., Vagnozzi S., Di Valentino E., Nunes R. C., Pan S., Mota D. F., 2019, *J. Cosmol. Astropart. Phys.*, 07, 037
- Yang W., Pan S., Mota D. F., Du M., 2020, *MNRAS*, 497, 879
- Zhang Y., Zhang H., 2021, *Eur. Phys. J. C*, 81, 706
- Zhang S., Cao S., Zhang J., Liu T., Liu Y., Geng S., Lian Y., 2020, *Int. J. Mod. Phys. D*, 29, 2050105
- Zhu L.-G., Hu Y.-M., Wang H.-T., Zhang J.-D., Li X.-D., Hendry M., Mei J., 2022, *Phys. Rev. Res.*, 4, 013247

This paper has been typeset from a $\text{\TeX}/\text{\LaTeX}$ file prepared by the author.